Supporting Information for:

Enhanced Oral Delivery of Protein Drugs Using Zwitterion-Functionalized Nanoparticles to Overcome both the Diffusion and Absorption Barriers

Wei Shan, [†] *Xi Zhu,* [†,‡] *Wei Tao,* [§] *Yi Cui,* [†] *Min Liu,* [†] *Lei Wu,* [†] *Lian Li,* [†] *Yaxian Zheng*[†] *and Yuan Huang*[†,*]

[†]Key Laboratory of Drug Targeting and Drug Delivery System, Ministry of Education, West China School of Pharmacy, Sichuan University, No. 17, Block 3, Southern Renmin Road, Chengdu 610041, China

[‡]National Shanghai Center for New Drug Safety Evaluation and Research, Shanghai, 201203, China

[§]School of life science, Tsinghua University, Beijing 100084, China

Corresponding Author

*E-mail: huangyuan0@163.com

Supporting Information Table S1.
Size and polydispersity index (PDI) of nanoparticles prepared with different phosphorylcholine derivatives*

Zwitterion-Lipid	Lipid/polymer ratio (%)	Solvent	Temp (°C)	Size (nm)	PDI
DLPC-1	10	DMSO	30	1487.6 ± 13.4	0.298
DLPC-2	20	DMSO	30	1057.3 ± 22.7	0.314
DLPC-3	30	DMSO	30	99.47 ± 4.0	0.133
DLPC-4	40	DMSO	30	88.9 ± 5.0	0.140
DMPC-1	10	THF	30	3789.4 ± 32.4	0.331
DMPC-2	20	THF	30	2364.7 ± 17.0	0.362
DMPC-3	30	THF	30	129.5 ± 1.4	0.233
DMPC-4	40	THF	30	175.9 ± 1.7	0.216
DOPC-1	10	DMF	30	8600.5 ± 2401.8	0.398
DOPC-2	20	DMF	30	3242.2 ± 65.8	0.422
DOPC-3	30	DMF	30	4577.5 ± 1117.0	0.403
DOPC-4	40	DMF	30	1746.3 ± 33.4	0.372
DSPC-1	10	DMSO	60	15294.3 ± 2435.2	0.675
DSPC-2	20	DMSO	60	10804.0 ± 6933.6	0.500
DSPC-3	30	DMSO	60	2562.3 ± 1389.7	0.585
DSPC-4	40	DMSO	60	29826.5 ± 19243.5	0.762
DPPC-1	10	DMSO	60	17981.1 ± 9032.2	0.864
DPPC-2	20	DMSO	60	13935.4 ± 8501.0	0.647
DPPC-3	30	DMSO	60	7468.5 ± 3749.7	0.491
DPPC-4	40	DMSO	60	1148.4 ± 175.4	0.338

*Measurements were taken after nanoparticles had been concentrated and re-suspended for 3 h in phosphate-buffered saline (mean ± SD, n= 3).

Supporting Information Table S2.
Entrapment efficiency and loading efficiency of NPs*

Sample	Entrapment efficiency (%)	Loading efficiency (%)
F127 NPs	16.5	4.4
PVA NPs	24.1	5.0
DLPC NPs	29.6	4.6

* Data are mean ± SD, n= 3.

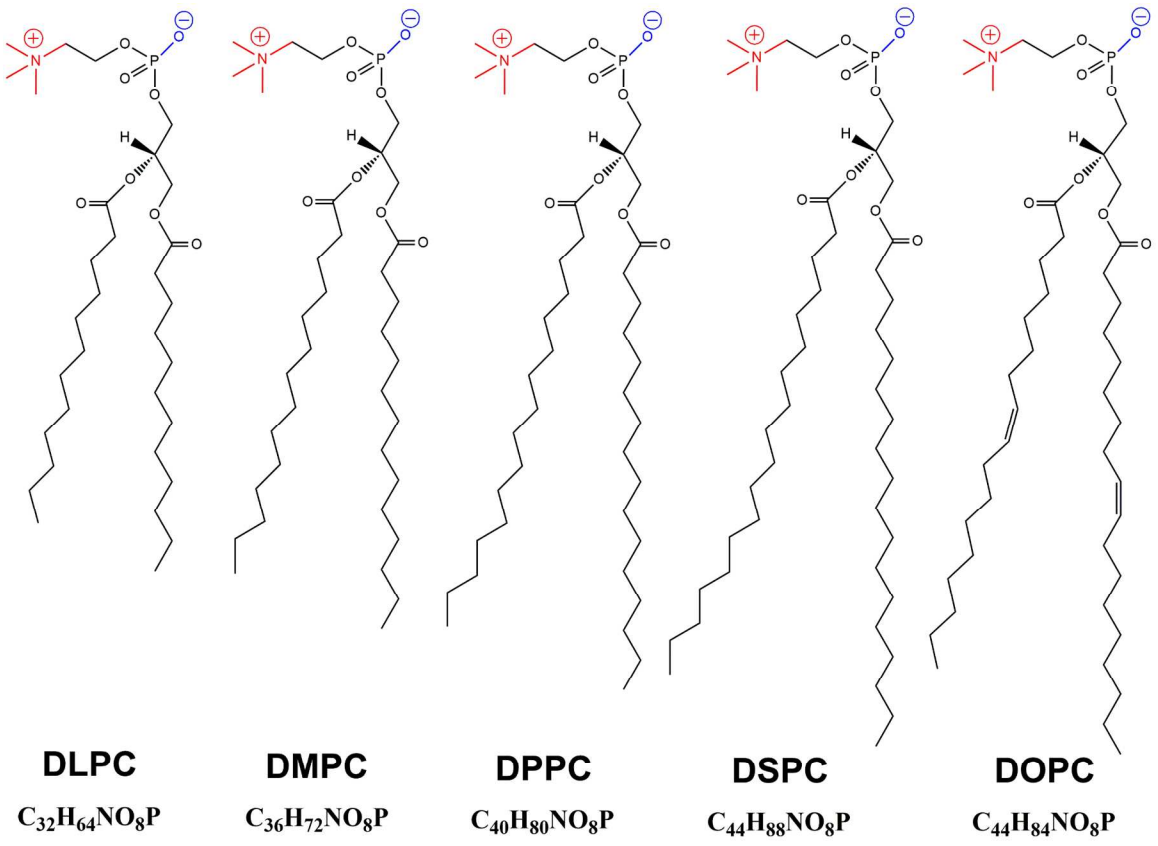

Supporting Information Figure S1. Chemical structures of lipid-zwitterions in this study.

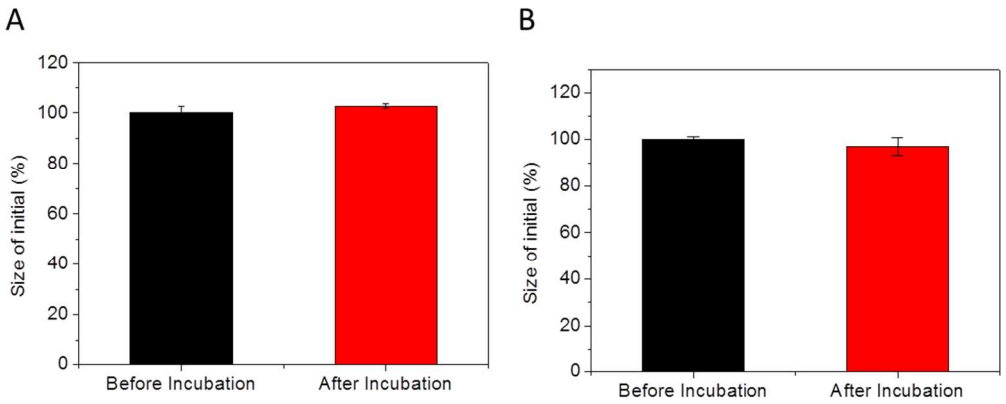

Supporting Information Figure S2. Colloidal stability of DLPC NPs after incubation with simulated gastric fluid (A) for 2 h and simulated intestinal fluid (B) for 6 h. Results were expressed as a percentage of the size before incubation (100%)

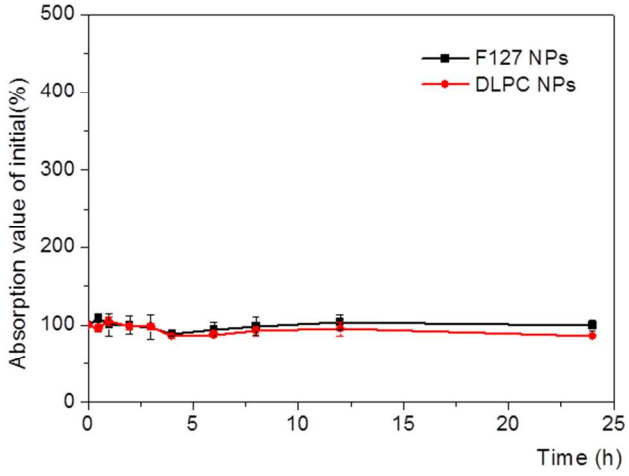

Supporting Information Figure S3. Turbidimetry of nanoparticle suspensions in 3 M NaCl buffered in phosphate buffer solution at 25 °C. Absorbance was measured at 500 nm and normalized to the value before incubation. Data are mean ± SD (n= 3).

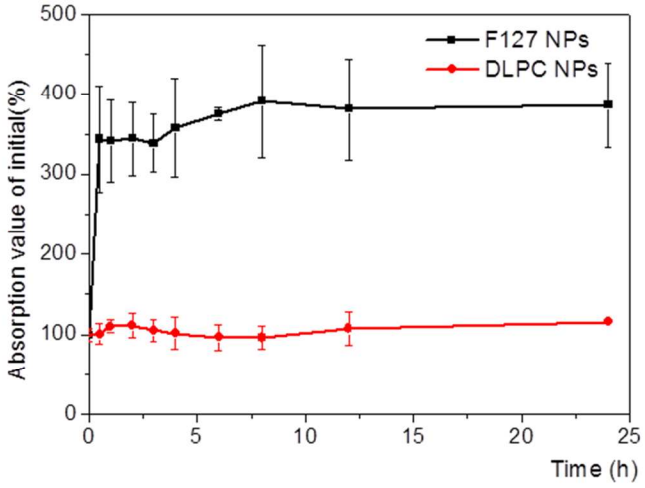

Supporting Information Figure S4. Turbidimetry of different NPs during incubation in 3 M NaCl buffered with PBS at 37°C. Absorption at 500 nm was measured and expressed relative to the value before incubation. Data are mean ± SD (n= 3).

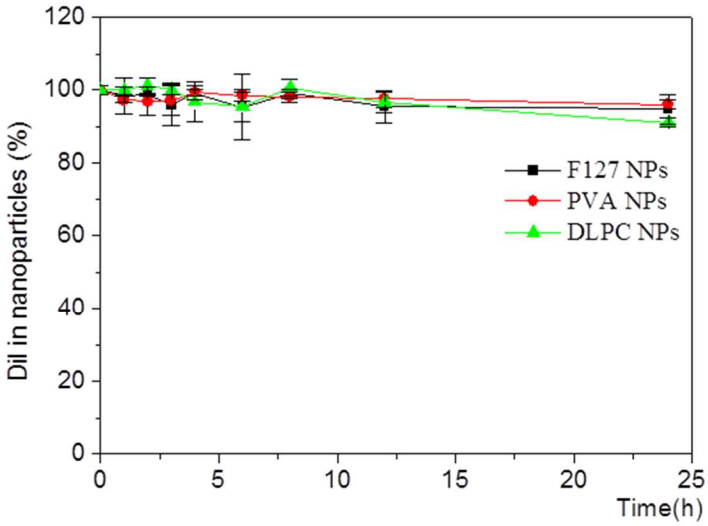

Supporting Information Figure S5. Release profile of Dil-loaded nanoparticles in phosphate-buffered saline (PBS, pH 7.4). Samples were dispersed in PBS and incubated at 37 °C with shaking at 100 rpm. At different times, aliquots (200 μl) were withdrawn and assayed for residual Dil. The amount remaining was expressed as a percent of the initial value before incubation (mean ± SD, n = 3).

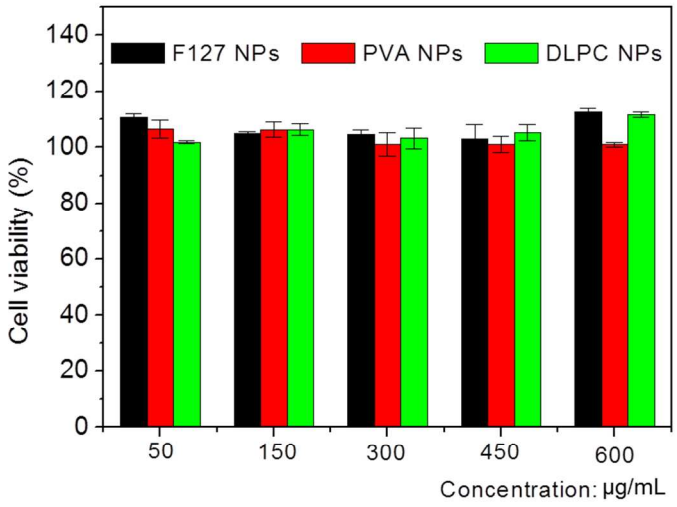

Supporting Information Figure S6. Viability of E12 cells after treatment with different formulations. Cells were co-incubated for 3 h with nanoparticles, the nanoparticles were removed, and cells were incubated a further 24 h. Cytotoxicity was evaluated using the Alamar Blue assay. Cells were incubated with Hank's balanced salt solution as a negative control. Viability was expressed as a percentage of the negative control (mean ± SD, n= 3).

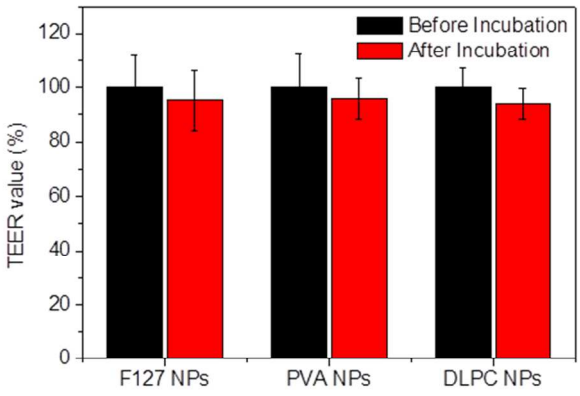

Supporting Information Figure S7. Transepithelial electrical resistance (TEER) of E12 cell monolayers before and after treatment with different nanoparticles. Values after incubation were expressed as a percentage of those before incubation (mean ± SD, n= 3).

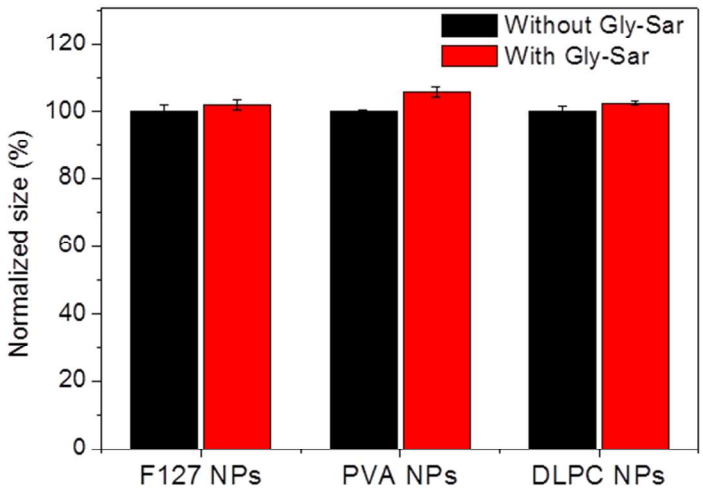

Supporting Information Figure S8. Influence of Gly-Sar on particle size of nanoparticles. Data were expressed as a percentage of the corresponding particles lacking Gly-Sar (mean ± SD, n= 3).

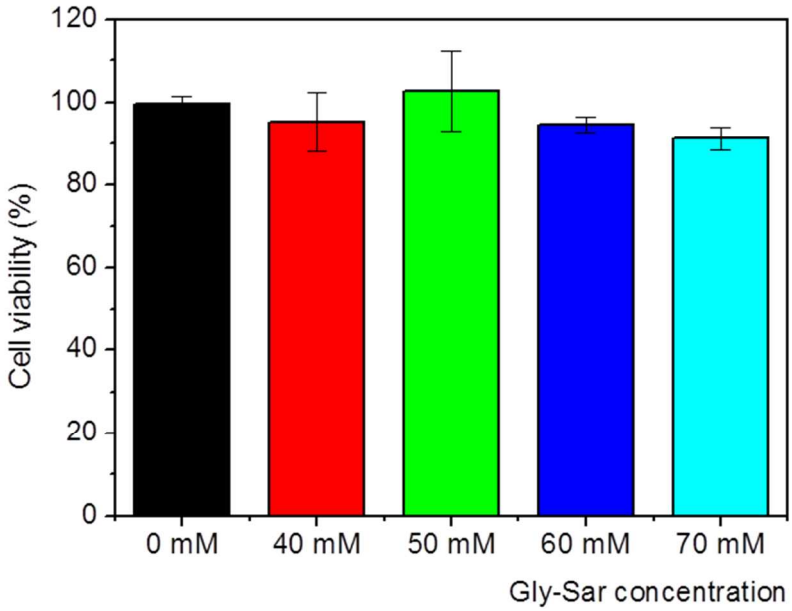

Supporting Information Figure S9. Viability of Caco-2 cells after treatment with different concentrations of Gly-Sar. Cells were co-incubated for 3 h with nanoparticles and Gly-Sar, nanoparticles were removed, and cells were incubated another 24 h. Cytotoxicity was evaluated using the Alamar Blue assay, and viability was expressed as a percentage of viability of negative control cells incubated only with Hank's balanced salt solution (mean ± SD, n = 3).

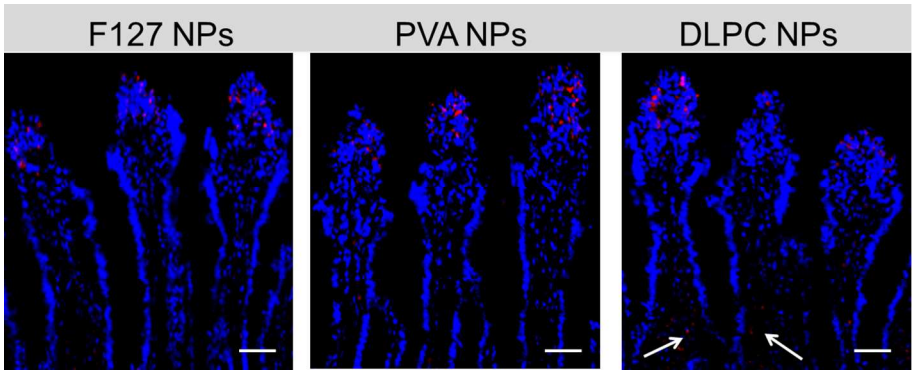

Supporting Information Figure S10. Representative fluorescence images of small intestine after local administration in rats. Scale bar, 50 μm. Arrows indicate NPs absorption into the interior of intestinal villi (red fluorescence).